1 # Electronic Supplementary Information

2 # Seed-assisted synthesis of a nanosheet-assembled
3 hierarchical SSZ-13 zeolite by coupling a small
4 amount of TMAdaOH with TPOAC

5

6 *Huifang Zhang [a], Qiuyu An [a], Feng Yu [a], Binbin Fan *[a]*

7 [a] College of Chemical Engineering and Technology, Taiyuan University of Technology,

8 Taiyuan 030024, P.R. China

9 * Corresponding authors: Binbin Fan

10 E-mail: fanbinbin@tyut.edu.cn

11

1 **S1. Experimental**

2 **S1.1. Chemicals**

3   Sodium hydroxide (NaOH, AR, 96%) was purchased from Kermel. Sodium aluminate

4 (NaAlO$_2$, CP) was obtained from Shanghai Test Chemical Reagents. *N,N,N*-trimethyl-1-

5 adamantanamine hydroxide (TMAdaOH, 25 wt% in water) was purchased from Energy

6 Chemical. Octadecyl-(3-trimethoxysilylpropyl)-ammonium chloride (TPOAC, 65 wt% in

7 water) and ammonium chloride (NH$_4$Cl, AR, 99.5%) were acquired from Macklin. Colloidal

8 silica (Ludox®HS-40) was purchased from Sigma-Aldrich. Potassium bromide (KBr),

9 aluminum isopropoxide (AR, 98%), fumed silica were purchased from Aladdin.

10 Chloroplatinate hexahydrate (H$_2$PtCl$_6 \cdot$6H$_2$O, 38-40% Pt) was obtained from J&K Scientific.

11 Distilled water is home made in the lab.

12 **S1.2. Synthesis of SSZ-13 Samples**

13   Synthesis of SSZ-13 seed. SSZ-13 seed was synthesized following the reported literature[1]

14 with some modifications. Specifically, 0.48 g NaOH and 10.2 g TMAdaOH were dissolved in

15 40 mL deionized water. Subsequently, 0.98 g aluminum isopropoxide was added and followed

16 by introducing 3.2 g fumed silica to the mixture. The resultant aluminosilicate gel (gel molar

17 composition was as follows: SiO$_2$: Al$_2$O$_3$: Na$_2$O : TMAdaOH : H$_2$O = 1 : 0.045 : 0.12 : 0.23 :

18 42) was stirred for 4 h at room temperature and transferred into a 100 mL Teflon-lined stainless-

19 steel autoclave and crystallized statically at 150 °C for 96 h. The recovered solid product was

20 washed, dried at 100 °C overnight and the dried solid powder was named as SSZ-13 seed.

21   Synthesis of SSZ-13-TP$_0$(r) and SSZ-13-TP$_{0.03}$(r) samples. The SSZ-13-TP$_0$(r) and SSZ-13-

1 $TP_{0.03}(r)$ samples with the different Si/Al ratios (5.5, 22, 33 and 55) were synthesized by

2 changing the amount of $NaAlO_2$ (0.6, 0.15, 0.1 and 0.06 g).

3   Synthesis of SSZ-13-TP_0-C and SSZ-13-$TP_{0.03}$-C. SSZ-13-TP_0-C and SSZ-13-$TP_{0.03}$-C were

4 synthesized in the synthesis system with $TMAdaOH/SiO_2 = 0.23$ in the absence or presence of

5 TPOAC. The detailed synthesis procedures of SSZ-13-TP_0-C and SSZ-13-$TP_{0.03}$-C are as

6 follows. 0.48 g of NaOH, 5.1 g of TMAdaOH and 0.3 g of $NaAlO_2$ were first dissolved into

7 14.5 mL of deionized water followed by stirring for 1 h at room temperature (in the absence or

8 presence of 0.55 g of TPOAC). Then, 0.16 g of SSZ-13 seed that previously synthesized was

9 added into the clear solution. Subsequently, 4 g of colloidal silica was slowly added and the

10 mixture was stirred for further 4 h. The resultant aluminosilicate gel (gel molar composition

11 was as follows: $SiO_2 : Al_2O_3 : Na_2O : TMAdaOH : TPOAC : H_2O = 1 : 0.045 : 0.28 : 0.23 : 0$ or

12 $0.03 : 42$) was transferred into a 50 mL Teflon-lined stainless-steel autoclave and crystallized

13 statically at 150 °C for 96 h. The product was washed and dried at 100 °C overnight. The

14 obtained sample were denoted as SSZ-13-TP_0-C and SSZ-13-$TP_{0.03}$-C, respectively.

15   Synthesis of SSZ-13-$TP_{0.03}$-N and SSZ-13-$TP_{0.03}$-CN. These samples were synthesized in

16 the absence of seed in the synthesis system with $TMAdaOH/SiO_2 = 0.04$ or 0.23, respectively.

17 ''N'' stands for the synthesis system in the absence of seed.

18   Synthesis of SSZ-13-C. SSZ-13-C was synthesized in the system with $TMAdaOH/SiO_2 =$

19 0.23 in the absence of TPOAC and seed. The detailed synthesis procedures are as follows. 0.48

20 g of NaOH, 5.1 g of TMAdaOH and 0.3 g of $NaAlO_2$ were first dissolved into 14.5 mL of

21 deionized water followed by stirring for 1 h at room temperature. Subsequently, 4 g of colloidal

1 silica was slowly added and the mixture was stirred for further 4 h. The resultant

2 aluminosilicate gel was transferred into a 50 mL Teflon-lined stainless-steel autoclave and

3 crystallized statically at 150 °C for 96 h. The product was washed and dried at 100 °C overnight.

4 The obtained sample were denoted as SSZ-13-C.

5 Synthesis of H-SSZ-13. H-SSZ-13 samples were prepared by ion-exchange method. H-SSZ-

6 13 sample (initial gel Si/Al ratio = 11) was ammonium-exchanged with 1 M NH_4Cl

7 (solid/liquid = 20) at 60 °C for 3 h for three times. The solid product recovered by filtering was

8 washed with distilled water for three times, dried at 100 °C overnight and calcined at 550 °C

9 for 6 h.

10 Preparation of Pt/SSZ-13 catalysts. Pt/SSZ-13 catalysts were prepared by impregnation

11 method. 266 μL of $H_2PtCl_6 \cdot 6H_2O$ solution (1g/50 mL) was added to 20 mL deionized water,

12 followed by adding 1 g of H-SSZ-13 to the above solution and stirring at 30 °C for 24 h. The

13 solvent was removed by rotary evaporation at 50 °C. The obtained solid was dried at 100 °C

14 overnight, calcined at 350 °C for 4 h in air and reduced at 350 °C for 2 h in H_2. The Pt contents

15 in all Pt/SSZ-13 catalysts were 0.2 wt.%. $0.2\%Pt/Al_2O_3$ and $0.2\%Pt/SiO_2$ were also prepared

16 by using the above impregnation method.

17 **S1.3.   Characterization**

18 Power X-ray diffraction (XRD) was tested on a Shimadzu XRD-6000 X-ray diffractometer

19 using Cu Kα radiation. Scanning electron microscopy (SEM) was recorded on a Hitachi S-

20 4800. N_2 adsorption/desorption was measured on a Quantachrome NOVA1200e. 0.05-0.1 g

21 sample was degassed under vacuum at 300 °C for 3 h prior to the adsorption measurements.

1   S_{mic} (micropore area) and V_{mic} (micropore volume) were calculated through the t-plot method.

2   S_{BET} (total surface area) and V_{tot} (total volume) were calculated using the BET equation and

3   DFT method, respectively. The contents of Si and Al were analyzed by a Thermo iCPA6300

4   inductively coupled plasma atomic emission spectrometer (ICP-AES). ^{27}Al MAS NMR spectra

5   were obtained at 156 MHz on a Bruker 600M spectrometer. The samples were spun at 12 kHz

6   using 4 mm rotors. Fourier transform infrared spectroscopy (FT-IR) spectra were collected on

7   a SHI-MADZU FTIR-Affinity-1 spectrometer. Temperature-programmed desorption of

8   ammonia (NH_3-TPD) was tested on a Tianjin Xianquan TP-5080D. 0.1 g sample was purged

9   with He at 500 °C for 2 h. After cooling down to 120 °C, 1%NH_3/He was flowed through the

10   sample for 1 h at a rate of 15 mL/min, and then purged with He for 0.5 h. Finally, the sample

11   was heated in He from 120 to 700 °C. The amount of NH_3 desorption was recorded by a TCD.

12   Transmission electron microscopy (TEM) was performed on a JEOL JEM-F200 to observe the

13   thickness of crystals and distribution of Pt NPs. H_2-pulse was conducted on a Sorb-91x to test

14   the dispersion of Pt NPs. 0.1 g sample was first reduced with 10% H_2/Ar at 350 °C for 1 h, and

15   then flushed with Ar at 350 °C for 1 h. After cooling down to 40 °C, 10% H_2/Ar was injected

16   into the U-tube reactor at regular intervals until the sample was saturated with H_2. X-ray

17   photoelectron spectroscopy (XPS) analysis of Pt 4d orbit was conducted on a Thermo Fisher

18   ESCALAB 250 xi spectrometer using Al Kα radiation. All spectra were calibrated utilizing the

19   C 1s peak at 284.8 eV.

20   **S1.4. Hydrogenation of naphthalene**

21   The liquid phase hydrogenation of naphthalene was conducted in a 50 mL stainless autoclave

1 reactor. The catalytic reaction was carried out by following the given procedure: 0.05 g of

2 milled catalyst, 5 mL of cyclohexane and 0.1 g of naphthalene were mixed and placed in the

3 autoclave reactor. After purification with H_2 for three times, the reactor was pressurized to 2

4 MPa and heated to 230 ℃ while stirring at 600 rpm. The collected liquid products were

5 analyzed on a gas chromatograph (Agilent 7820A) with an HP-5 capillary column (30 m × 0.32

6 mm × 0.25 μm).

7

8   **Table S1** BET and textural parameters of SSZ-13 samples

| Sample	S_{BET}	S_{mic}	S_{ext}	V_{tot}	V_{mic}	V_{meso}
	$(m^2 \cdot g^{-1})$	$(m^2 \cdot g^{-1})$	$(m^2 \cdot g^{-1})$	$(cm^3 \cdot g^{-1})$	$(cm^3 \cdot g^{-1})$	$(cm^3 \cdot g^{-1})$
SSZ-13-TP$_0$(22)	792	752	40	0.38	0.29	0.09
SSZ-13-TP$_0$(33)	766	733	33	0.36	0.28	0.08
SSZ-13-TP$_{0.03}$(22)	778	707	71	0.40	0.27	0.13
SSZ-13-TP$_{0.03}$(33)	793	722	71	0.45	0.27	0.18
SSZ-13-TP$_0$-C	668	625	43	0.33	0.23	0.10
SSZ-13-TP$_{0.03}$-C	655	553	102	0.50	0.21	0.29
SSZ-13-C	706	673	33	0.33	0.25	0.08
SSZ-13-TP$_{0.015}$	759	714	45	0.40	0.27	0.13
SSZ-13-TP$_{0.06}$	721	640	81	0.42	0.24	0.18

9

10

1 **Figures**

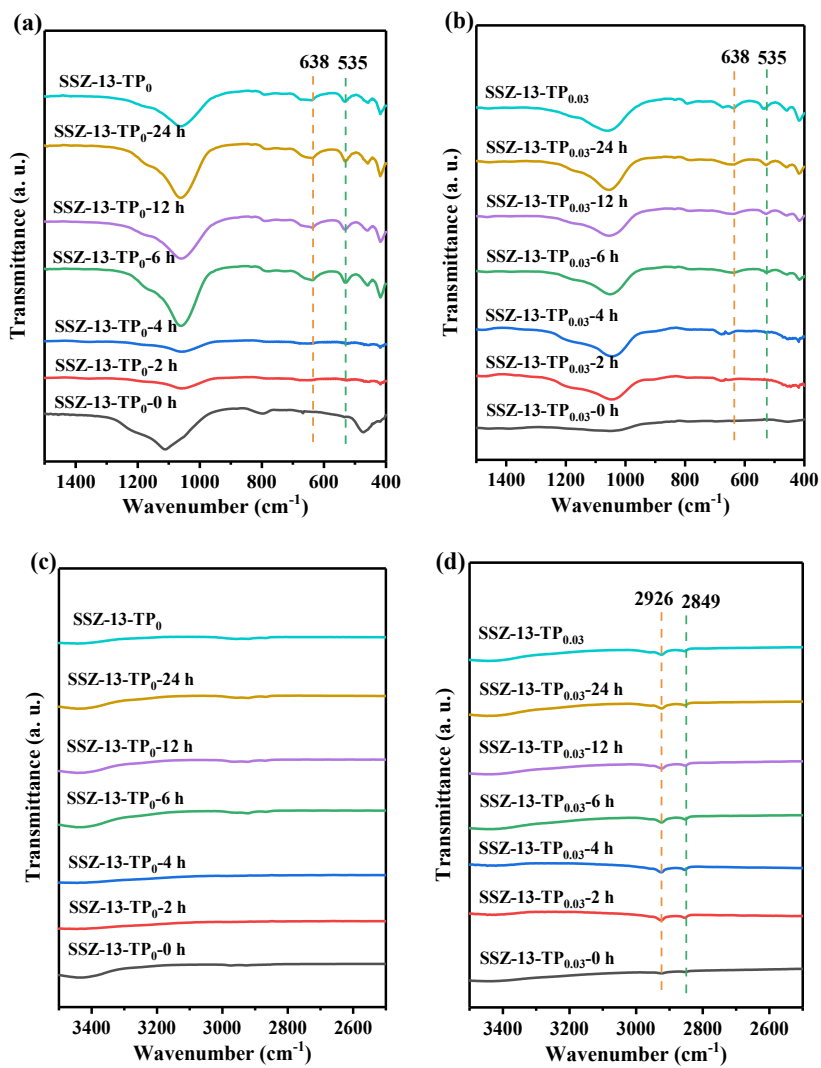2 **Fig. S1** XRD pattern and SEM image of SSZ-13 seed.

3 **Fig. S2** SEM images of SSZ-13-TP$_0$-y h and SSZ-13-TP$_{0.03}$-y h samples.

4 **Fig. S3** FT-IR spectra of (a and c) SSZ-13-TP$_0$-y h and (b and d) SSZ-13-TP$_{0.03}$-y h samples.

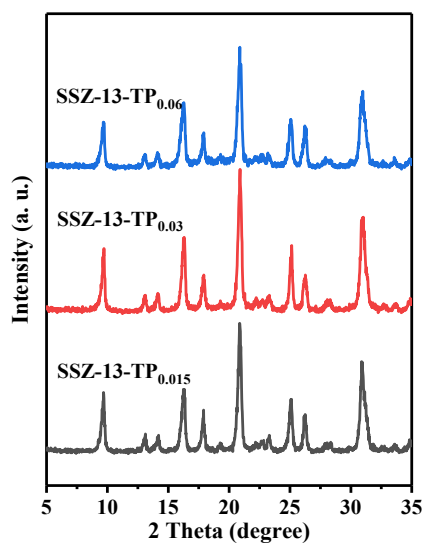5 **Fig. S4** XRD patterns SSZ-13-TP$_0$(r) and SSZ-13-TP$_{0.03}$(r) samples.
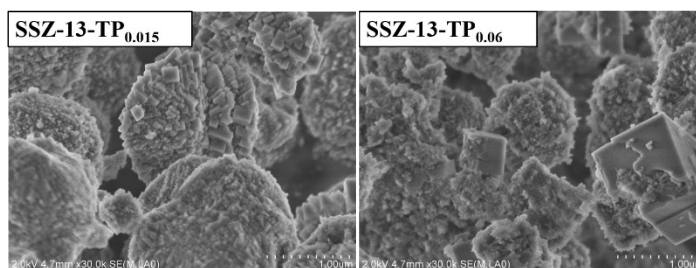
6 **Fig. S5** SEM images of SSZ-13-TP$_0$(r) and SSZ-13-TP$_{0.03}$(r) samples.

7 **Fig. S6** XRD patterns of SSZ-13-TPx samples.

8 **Fig. S7** SEM images of SSZ-13-TPx samples.

9 **Fig. S8** XRD patterns of SSZ-13-TP$_0$-C and SSZ-13-TP$_{0.03}$-C.

10 **Fig. S9** XRD patterns of SSZ-13-TP$_{0.03}$-N and SSZ-13-TP$_{0.03}$-CN.

11 **Fig. S10** XRD pattern of SSZ-13-C.

12

13
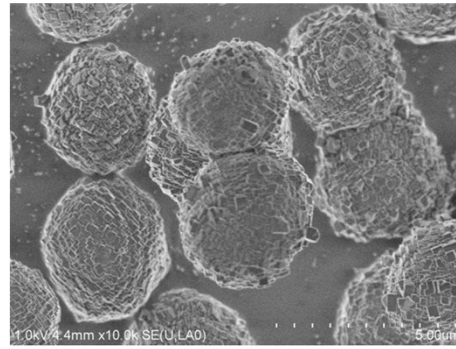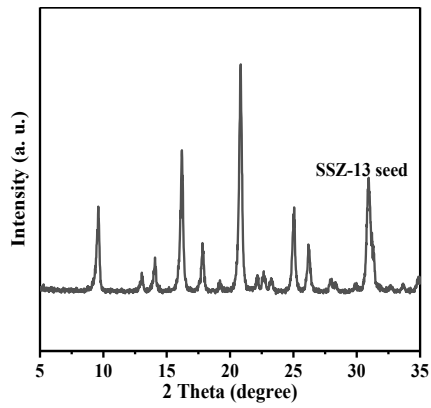
1

2   **Fig. S1** XRD pattern and SEM image of SSZ-13 seed.
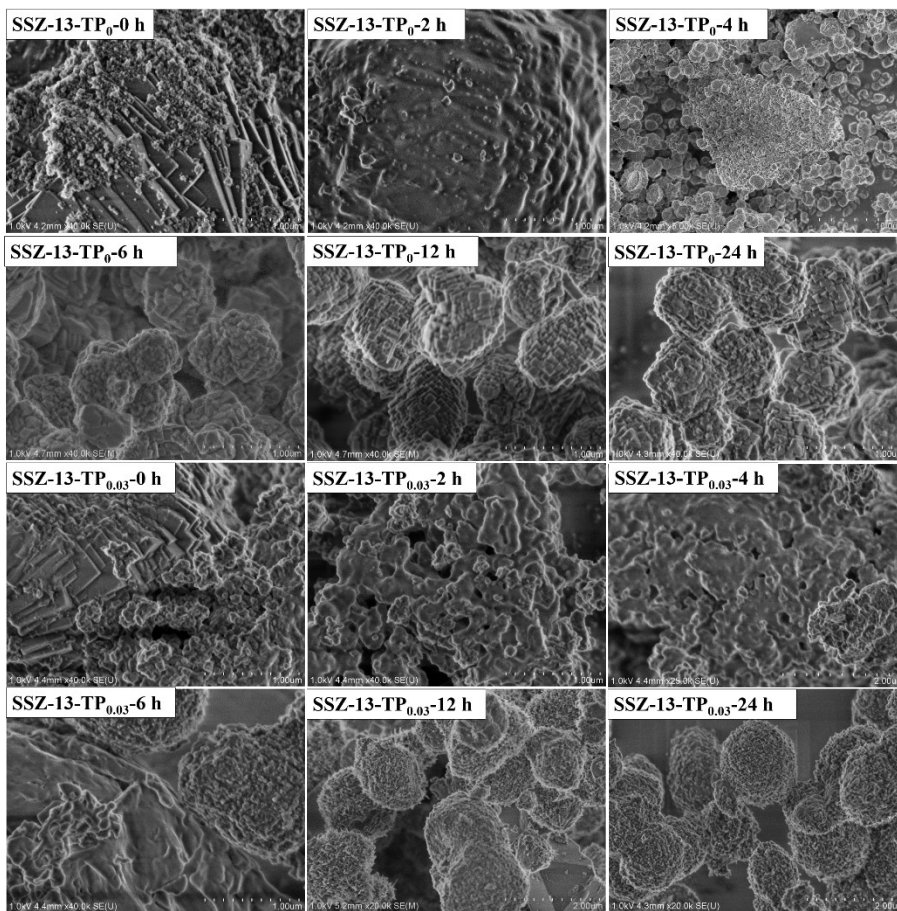
3

4   **Fig. S2** SEM images of SSZ-13-TP$_0$-y h and SSZ-13-TP$_{0.03}$-y h samples.

5

Fig. S3 FT-IR spectra of (a and c) SSZ-13-TP$_0$-y h and (b and d) SSZ-13-TP$_{0.03}$-y h samples.
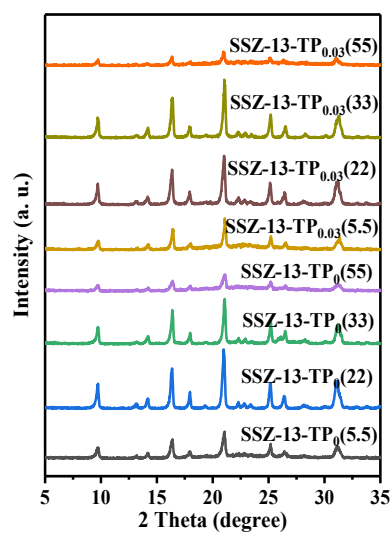
Fig. S4 XRD patterns SSZ-13-TP$_0$(r) and SSZ-13-TP$_{0.03}$(r) samples.
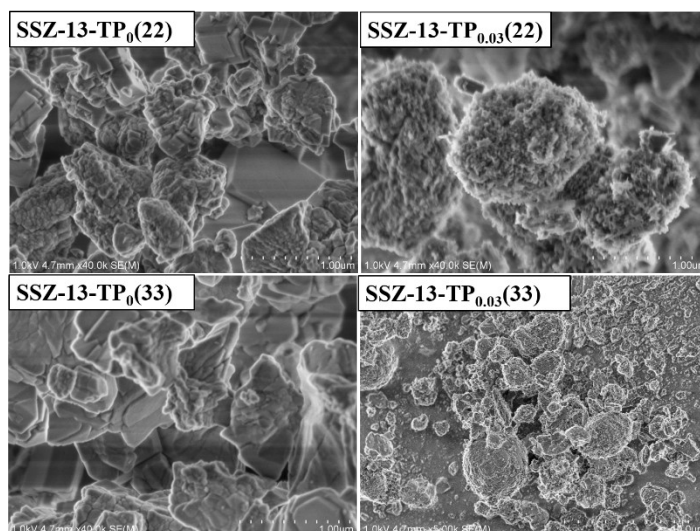
1

2 **Fig. S5** SEM images of SSZ-13-TP$_0$(r) and SSZ-13-TP$_{0.03}$(r) samples.

3

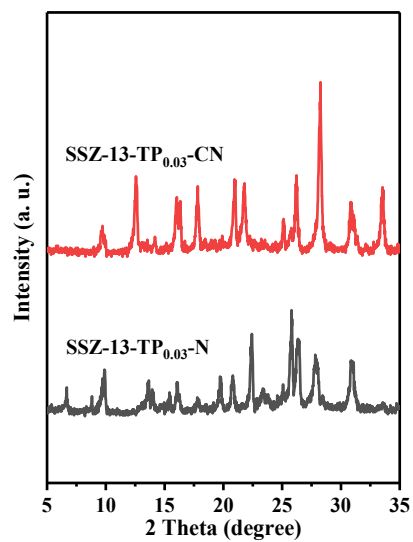4 **Fig. S6** XRD patterns of SSZ-13-TPx samples.
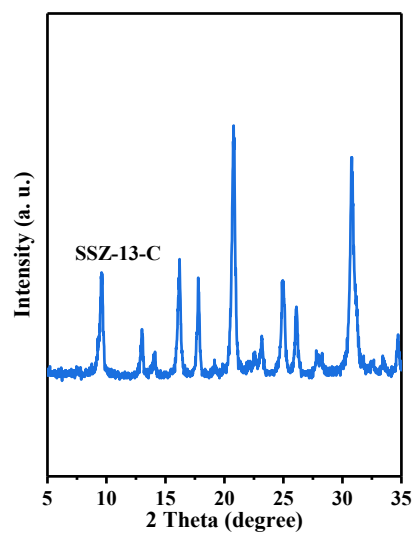
5

6 **Fig. S7** SEM images of SSZ-13-TPx samples.
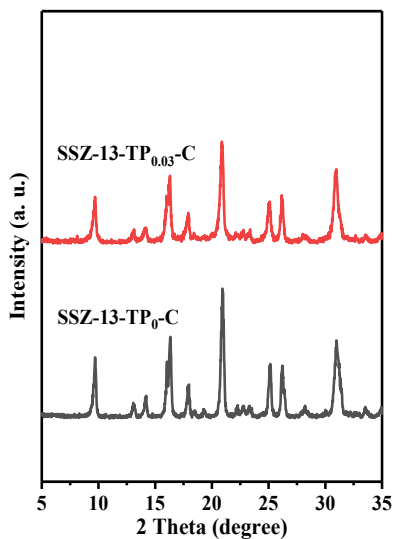
Fig. S8 XRD patterns of SSZ-13-TP$_0$-C and SSZ-13-TP$_{0.03}$-C.

Fig. S9 XRD patterns of SSZ-13-TP$_{0.03}$-N and SSZ-13-TP$_{0.03}$-CN.

Fig. S10 XRD pattern of SSZ-13-C.

Reference

1 Z. Xu, J. Li, Y. Huang, H. Ma, W. Qian, H. Zhang and W. Ying, *Catal. Sci. Technol.,* 2019, **9,** 2888–2897.